INVESTIGATION OF NANOCERIA-MODIFIED PLATINUM-GOLD COMPOSITE ELECTRODES FOR THE ELECTROCHEMICAL REDUCTION OF OXYGEN IN ALKALINE MEDIA

by

RAHUL HEGISHTE
M.Sc. University of Pune, India, 2001
B.Sc. University of Mumbai, India, 1999

A thesis submitted in partial fulfillment of the requirements
for the degree of Master of Science
in the Department of Chemistry
in the College of Sciences
at the University of Central Florida
Orlando, Florida

Spring 2011

© 2011 Rahul Hegishte

ABSTRACT

Platinum-gold and nanoceria-modified platinum-gold electrodes were prepared on a platinum surface via electrochemical reduction of solutions of platinum and gold salts in the dispersion of nanoceria. The molar ratios of Pt and Au were varied in both PtAu and PtAu/CeO_2 electrodes while the total concentration of the metals was maintained at 2 x 10^{-3}M and the concentration of nanoceria was maintained constant at 5 x 10^{-3}M. The electrodes were characterized by their cyclic voltammetry curves in 0.5M sulfuric acid solution. The electrochemically active area of the electrodes was determined using the copper underpotential deposition method. The linear sweep voltammograms of the PtAu and PtAu/CeO_2 electrodes were plotted from -1V to 0V vs. Ag/AgCl, 3M KCl reference electrode using the rotating disk electrodes for the rotation speeds from 200 to 3600rpm in an oxygen saturated 0.1M sodium hydroxide solution. The values of the kinetic controlled current density were determined from the rotating disk voltammetry. The values of the limiting current density for each rotation speed were used to plot the Koutecky-Levich plots for the electrodes. The rate constants were obtained from the Koutecky-Levich plots for each composition of the electrode. The values of kinetic current density and the rate constants indicated that the addition of Au enhances the ORR rates in both the PtAu and the PtAu/CeO_2 electrodes. The values of the kinetic current densities of the PtAu/CeO_2 were lower than that of the PtAu electrodes owing to the poor electrical conductivity of ceria. The Koutecky-Levich plots for the PtAu and the PtAu/CeO_2 electrodes are linear for the four-electron reduction of oxygen in the alkaline media, which indicates that the overall reaction follows the first order kinetics. The electron transfer rate constants obtained from the Koutecky-Levich plots for the PtAu and the PtAu/CeO_2 electrodes both were found to increase in values with the addition of

Au. The Tafel plots were plotted for the PtAu and PtAu/CeO_2 electrodes and the values of Tafel slopes were found to be in a small range for lower amounts of Au which indicated that the ORR rates were enhanced in lower amounts of Au. The values of Tafel slopes were found to be much higher for the ceria-modified PtAu electrodes as compared to the PtAu electrodes, which indicate the lower rates of ORR after the modification with ceria. Also, the ORR rates for the electrodes with smaller amounts of Au in PtAu/CeO_2 were higher than those in the larger amounts of Au.

To my parents who are the pillars of my life. Without you, my life would fall apart. Your teachings and moral values gave me the inspiration to learn, work hard and become strong. Special thanks to my mother for her faith in me and for her teaching that I should never surrender. Thanks to my father who invested in me so much and supported me in every situation in my life.

ACKNOWLEDGMENTS

I am indeed thankful to my advisor, Dr. Diego J. Diaz, whose inspiration and constant encouragement made this thesis possible. I am also thankful to him for having given me an opportunity to explore in his research group and for giving his valuable time and taking interest in my learning the subject of electrochemistry. I am also thankful to the fellow students in the research group of Dr. Diaz for their experimental assistance and discussions.

I am thankful to the Department of Chemistry at the University of Central Florida (UCF) for giving me an opportunity to learn and contribute to the research as a graduate student. I am also thankful to the Graduate Program for giving me an opportunity to teach as a Graduate Teaching Assistant (GTA) for the last several years. I am thankful to the faculty of the Chemistry Department with whom I took the courses. I am also thankful to the faculty with whom I had the opportunity of working as a GTA and learn indeed wonderful techniques in teaching and research.

I am thankful to my friends, well-wishers and roommates whom I met during my graduate study at UCF for their moral support, motivation and for cheering me up especially during hard times.

I cannot forget to thank my parents who allowed me to continue my studies and stood besides me firmly in all the ups and downs that came across my way and never ceased to bless me at every moment and in every situation.

TABLE OF CONTENTS

LIST OF FIGURES

LIST OF TABLES

LIST OF ABBREVIATIONS

CV	Cyclic voltammetry
ECA	Electrochemically active area
LSV	Linear sweep voltammetry
ORR	Oxygen reduction reaction
PEM	Polymer electrolyte membrane
PEMFC	Polymer electrolyte membrane fuel cell
RDE	Rotating disk electrodes
upd	Under-potential deposition

CHAPTER 1. INTRODUCTION

The invention of fuel cells as an electrical energy conversion system is attributed to Sir William Grove [1]. In 1839, he developed the first electrochemical energy conversion technology known to man. The field has advanced so much that the fuel cells of the present day, such as the hydrogen fuel cells and methanol fuel cells are of huge economic interest, and are currently under high attention for the large-scale commercialization as the future energy devices [1]. The space program which begun in the mid 20th century had very special requirements of the fuel to be used for the spaceships and was most benefited from the development of the fuel cells [2]. The ever increasing demand for energy and the fast depleting nature of the existing natural energy sources such as coal, petroleum, natural oil which are limited in their reserves, makes it necessary for mankind to explore newer sources of energy.

1. Fuel cells

Fuel cells are energy conversion devices in which the chemical energy is converted into electrical energy. The most striking advantages which make the fuel cells unique and popular are that they are renewable and portable [1]. The fuels such as methanol, ethanol, for example, are generated from the sources such as biofuel, which are renewable in nature. The fuel cells can be used as energy sources in many portable devices such as laptop computers, mobile phones, GPS systems, for example a few and have many potential applications in the future.

In a fuel cell, the electricity is generated through the oxidation of a fuel at the anode and the reduction of an oxidant, typically oxygen at the cathode. The anode and the cathode are separated by an electrolyte. Based on the kind of the electrolyte medium used, the fuel cells can

be classified into various types such as polymer electrolyte membrane fuel cell (PEMFC), solid oxide fuel cell (SOFC), alkaline fuel cell (AFC), phosphoric acid fuel cell (PAFC) and molten carbonate fuel cell (MCFC) among others [3].

In a PEMFC, a semi-permeable polymer membrane which separates the anode and cathode acts as the electrolyte. The polymer electrolyte membrane (PEM) consists of several layers of thin sheets of polymer such as Nafion ® (sulfonated tetrafluoroethylene based fluoropolymer-copolymer), for example, stacked such that they act as the medium for the selective conduction of protons through the membrane. The PEM facilitates the exchange of protons between the two electrodes. PEMFCs are low-temperature fuel cells, generally operating between 85 – 105^{o}C. The typical fuels used in the PEMFCs are hydrogen, methanol, ethanol or formic acid. For example, when hydrogen is used as a fuel, the half-cell reactions are as follows:

Anode half-reaction: $2\ H_2 \rightarrow 4\ H^+ + 4\ e^-$ $E^0 = 0.00V$ (1)

Cathode half-reaction: $O_2 + 4\ e^- + 4\ H^+ \rightarrow 2\ H_2O$ $E^0 = 1.23V$ (2)

Overall cell reaction: $2\ H_2 + O_2 \rightarrow 2\ H_2O$ $E^0 = 1.23V$ (3)

The half-reaction at the anode involving hydrogen oxidation, is facile with the present day platinum-based catalysts [4 - 6].

The half-reaction at the cathode which is the four-electron reduction of oxygen to water, also called as oxygen reduction reaction (ORR), is however, not facile, even with a platinum catalyst. The difficulty in oxygen reduction lies in the exceptionally strong O=O bond (498kJ/mol). The activation of this bond is kinetically slow which results in high overpotential for the oxygen reduction reaction (ORR) and hence a low performance of the cathode, which in turn affects the overall energy efficiency of a fuel cell. A tremendous amount of research effort has already been

done over last few decades in developing a suitable catalyst which can improve the performance of the ORR at the cathode and is still a subject of high attention in the scientific and technological field, which mainly includes the energy conversion devices such as the fuel cells and batteries.

The choice of developing a catalyst for improving the performance of ORR at the cathode of the fuel cell was made by our research group with an intention of contributing towards this really important and crucial problem in the field. We have recently studied the performance of $PtAu/CeO_2$ catalyst for the anode of direct methanol fuel cell using electrodeposition technique [7] for preparing the electrode. The knowledge of the electrodeposition technique will facilitate the preparation of the catalyst for the cathode of the fuel cell.

2. Oxygen reduction reaction (ORR)

The oxygen electrochemistry is of high importance in the field of electrocatalysis, especially due to its application in electrochemical energy conversion technologies such as in fuel cells and batteries [8]. A large amount of R&D effort in fuel cell technology especially in the last two decades has led to numerous studies on the ORR on various materials and they encompass a wide range from noble metals over transition metal oxides to organic macrocycles. Several reviews have been published on the materials for the catalyst for ORR so far [9 - 11]. Platinum has been the metal of choice for the ORR catalyst in most of the studies because of its comparatively high electrocatalytic ability and chemical stability among the transition metals studied. The use of Pt as the material for the catalyst at the cathode is restricted by its huge cost and hence the ways to find a replacement for Pt or to reduce its content has become increasingly important.

The catalytic ability of Pt towards ORR has been found to be enhanced by the development of binary Pt alloys such as PtNi, PtCo, PtFe, to mention a few [9, 12 – 15]. The metal added in small amounts to Pt has been shown to improve the performance of the catalyst towards ORR. The added metal such as Co, for example, reduces the formation of Pt-OH bond and facilitates the faster reduction of $Pt\text{-}O^{-}$. The ORR process was found to take place mainly by a four-electron reduction pathway.

Even though the binary catalysts showed improved ORR performance compared to a Pt/C catalyst, their stabilities were found to be still poor. The addition of transition metal oxides into the cathode has been studied to facilitate the supply of oxygen species leading to the enhanced fuel cell performance [16 – 23]. The oxides such as zirconia, for example, not only improve the ORR activity but also impart stability to the Pt, Au based catalysts in the acidic solutions. The titania has been shown to improve the durability of the ORR catalyst mainly by preventing the dissolution or segregation in addition to enhancing the performance of the catalyst towards ORR. In addition to these, some ceramic materials such as tin oxide, doped SnO, silica, ruthenium oxide, tungsten oxide, indium tin oxide and several inorganic oxides have been found to impart good stability and act as good support materials for the ORR catalysts. Among the various transition metal oxides studied so far, ceria has been found to exhibit a positive catalytic synergy owing to its ability to store and release oxygen [24]. Ceria is a fluorite-structured oxide with high oxygen storage capacity associated with its rich oxygen vacancies and low redox potential between Ce^{3+} and Ce^{4+}. Our group has recently studied the ability of ceria in improving the electrooxidation of ethanol and methanol [7, 25].

The carbon-supported platinum (Pt/C) catalyst has been reported to yield a good level of performance towards ORR [26]. The ORR has been found to follow mainly a direct four-electron reduction pathway on Pt/C catalyst. The effect of the introduction of ceria nanoparticles into the Pt/C catalyst towards the ORR was studied by Lim, D., et al [27]. Their study confirms the oxygen storage and releasing ability of ceria in the catalyst. Another remarkable part of their findings is the increased durability and stability of the Pt-CeO_2/C in the electrolyte media as compared to that of the commercially available Pt/C catalyst. The release of oxygen by ceria can be explained by the $Ce^{3+} – Ce^{4+}$ redox equilibrium and can be given by the following equation:

$$2\ CeO_2 \rightleftharpoons Ce_2O_3 + \tfrac{1}{2}\ O_2 \qquad (4)$$

3. ORR in acidic and alkaline media

Most of the fundamental studies of the ORR have been conducted in acidic electrolyte [28 - 30]. This is primarily because the acid electrolytes are mainly used in the fuel cells. The polymer electrolyte membrane such as Nafion ®, for example, used in PEMFCs is also acidic in nature. The main advantage of studying the ORR in the alkaline media is that it exhibits a lower overpotential in the alkaline media than in the acidic media [31]. In the potential region from 0.595 to 0.395 V vs. Ag/AgCl, 3M KCl reference, the kinetics of ORR has been found to decrease in the electrolytes in the order: $KOH > H_2SO_4 \approx CF_3SO_3H > H_3PO_4 > HClO_4$ [31]. The minimal adsorption of the OH^- ion largely contributes to the superior ORR performance of the catalysts in KOH. However, the low solubility of oxygen in alkali as compared to that in acid, and the CO_2 rejection are a few known disadvantages. The low solubility of oxygen, on the other hand, can be compensated by supporting the catalysts with the transition metal oxides, such as

ceria, for example, which can release oxygen in the electrolyte medium and maintain an optimum concentration of oxygen at the electrode. The electrocatalysis of the ORR in the alkaline media is also of interest because of its applications in chlor-alkali electrolysis with air-depolarized cathodes [32, 33], as well as in metal-air batteries [34, 35], and also because of its relevance to corrosion processes [36 - 38].

The overall reaction of oxygen reduction in the alkaline media is given as follows:

$$O_2 + 2\ H_2O + 4\ e^- \rightarrow 4\ OH^- \quad (5)$$

The mechanism for the ORR in the alkaline media has been given by Yeager, E. [39], as follows:

$$O_2 + H_2O + 2\ e^- \rightarrow HO_2^- + OH^- \quad (6)$$

$$HO_2^- + H_2O + 2\ e^- \rightarrow 3\ OH^- \quad (7)$$

$$2\ HO_2^- \rightarrow 2\ OH^- + O_2 \quad (8)$$

The possible pathways of the ORR on a catalyst surface in the alkaline media have been given in the mechanism shown in figure 1 [40].

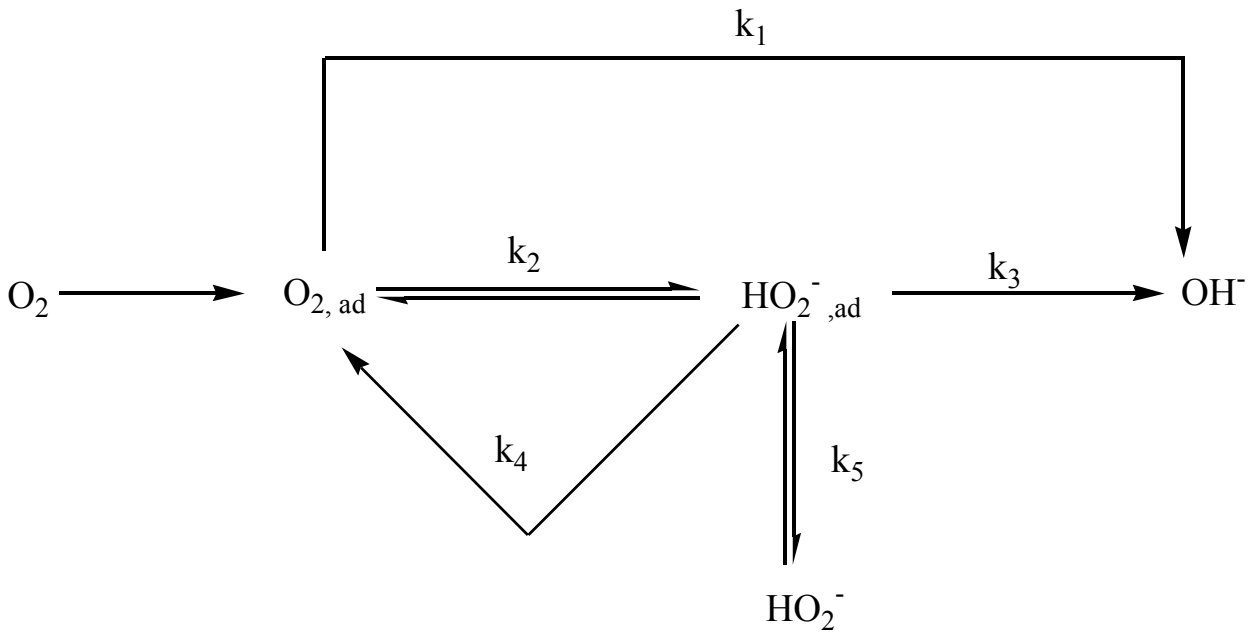

Figure 1: Mechanism of ORR on a catalyst surface in alkaline media

The catalysis begins with the adsorption of O_2 gas on the Pt-surface. The adsorbed O_2 ($O_{2,\,ad}$) on the electrode can react either via 4-electron reduction path to form OH^-, denoted by k_1-path, or follow a serial pathway through the intermediate formation of adsorbed $HO_2^-{}_{,ad}$, denoted by k_2-path. The $HO_2^-{}_{,ad}$ can be further reduced to OH^- denoted by k_3 path. This is a 2 + 2 e^- - reduction represented by equations (6), (7) in the ORR mechanism.

The $HO_2^-{}_{,ad}$ species can desorb from the electrode to the solution phase (k_5-path). Also, $HO_2^-{}_{,ad}$ can chemically decompose to form water and O_2 back in a heterogeneously catalyzed reaction step (k_4-path).

It has been found that the ORR on Pt follows the serial reaction (i.e. 2 + 2 e^- - reduction) pathway through the formation of $HO_2^-{}_{,ad}$ (k_1 is negligible), but without producing any detectable amounts of HO_2^- in solution, i.e. $k_3 >> k_5$.

4. Choice of the catalyst

The study on the development of PtAu based catalysts for ORR has been done by several groups so far. The PtAu–modified C-TiO_2 composites prepared using photodeposition [41], modified PtAu nanoparticles prepared using chemical synthesis [42], modified core-shell PtAu catalyst prepared using successive reduction [43] are some of the several methods in which the modified PtAu catalysts have been prepared and studied for their performance towards ORR. In most of the studies, the addition of Au in Pt has shown to synergize the activity of the catalyst towards ORR. The addition of Au atoms to the Pt catalysts has also been found to increase the stability of the catalyst towards dissolution. To the best of our knowledge, the electrocatalytic ability of nanoceria-modified PtAu (PtAu/CeO_2) composite [44, 45] prepared via the electrochemical reduction of the Pt, Au salts in the dispersion of nanoceria towards ORR in the alkaline media has not been reported and was chosen for this study. The experiments were aimed at studying the effect of increase of Au in the Pt catalyst and also at studying the effect of introducing nanoceria in the PtAu alloy towards ORR in the alkaline media.

5. Electrochemical techniques

Electrochemistry is a field of chemistry that deals with the chemical phenomena associated with charge transfer which can occur homogeneously in solution, or heterogeneously on electrodes. The knowledge of electrochemistry allows the study of the chemical changes caused by the passage of an electric current and the interaction of electrical energy with the chemical reactions. The basic principles of electrochemistry cover a large variety of different phenomena. The main focus here is on the application of electrochemical methods to the study of the surface

characteristics of the catalysts and the rates of the oxygen reduction reaction to which they are employed.

Cyclic voltammetry

Cyclic voltammetry (CV) is a potentiodynamic electrochemical technique in which a linear sweep in the potential is applied [46]. As the potential is increased or decreased, the value for the potential will reach the threshold in which electrochemical oxidation or reduction will occur, generating a large increase or decrease in the current respectively. In general, CV provides information about the thermodynamic and kinetics of the processes that occur on the electrode/electrolyte interface. The total amount of charge, which can also be defined as the integration of that generated current over a period of time, which is defined by the rate of the linear sweep in potential, is directly related to the amount of the species oxidized. In a CV, the direction of the applied potential can be reversed. The positive direction of the potential which is termed as the anodic direction is followed by the negative direction which is termed as the cathodic direction and it is repeated for a number of cycles.

Linear sweep voltammetry

Linear sweep voltammetry is a voltammetric method where the current at a working electrode is measured while the potential between the working electrode and a reference electrode is swept linearly in time in either anodic or cathodic direction [46]. The oxidation or reduction of the species is registered as a peak or trough in the current signal at the potential at which the species begins to be oxidized or reduced respectively. The current vs. voltage (I – V) curve that is obtained gives information about the electron transfer processes that are occurring at the

electrode-solution interface. This technique is useful for investigating the electron transfer steps involved in the multi-step processes.

Rotating disk electrodes

The nature of the study using the rotating disk electrodes (RDE) is similar in nature to the CV studies [46]. In CV studies, the solution is kept non-stirred and the mass transport is limited by the diffusion of material into the electrode. The slower process in a chemical reaction determines the overall rate of the reaction. Hence, it limits our ability to provide the information on the kinetics of the electron transfer as enhanced by a catalyst.

In RDE, the working electrode is rotated in solution as the linear sweep in the potential is applied. By controlling the rate of rotation of the electrode, the hydrodynamic mass transport is generated, thereby removing the mass transport limitations on the current. A value for the rotation can be reached such that enough material is brought to the electrode that the current will be limited by the ability to undergo the redox reaction in the time allowed by the mass transport. The limiting current obtained in a RDE experiment is a contribution from the electron transfer process and the diffusion of the species towards the electrode surface.

Koutecky-Levich plot

The relation between the limiting current of the species involved in the electrode process to its kinetic and diffusion controlled parts is given by the Koutecky-Levich equation [46]:

$$\frac{1}{I} = \frac{1}{I_k} + \frac{1}{I_d} \qquad (9)$$

where I_k is the kinetic (electron transfer) current, and I_d is the diffusion current.

The kinetic current I_k is given by:

$$I_k = nFk_f C \qquad (10)$$

where n is the number of electrons transferred per molecule, F is the Faraday's constant (F = 96,485 $Cmol^{-1}$), k_f is the electron transfer rate constant (cms^{-1}), and C is the bulk concentration of the redox species ($moldm^{-3}$).

The diffusion current is given by:

$$I_d = 0.620nFCD^{2/3}v^{-1/6}\omega^{1/2} \qquad (11)$$

where D is the diffusion coefficient (cm^2s^{-1}), v is the kinematic viscosity of the solution (cm^2s^{-1}) and ω is the rate of rotation of the disk electrode in rad/s.

The equations (9), (10) and (11) can be combined together to give the following equation:

$$\frac{1}{I} = \frac{1}{nFk_f C} + \frac{1}{0.620nFCD^{2/3}v^{-1/6}\omega^{1/2}} \qquad (12)$$

The plot of the reciprocal of the current density vs. reciprocal of the square-root of the rotation rate, i.e. I^{-1} vs. $\omega^{-1/2}$ will be a straight line plot whose intercept will be equal to $1/nFk_fC$. This plot is called as Koutecky-Levich plot. The knowledge of the number of electrons transferred allows us to calculate the value of the electron transfer rate constant (k_f) and vice-versa, the value of the rate constant allows the calculation of the number of electrons transferred in the reaction.

The application of Koutecky-Levich plots can be used to study the number of electrons transferred and the heterogeneous rate constants in the one-step and multi-step electron transfer reactions at the rotating disk electrodes. Also, the information obtained from using the Koutecky-Levich plots can assist in studying the mechanisms of several types of electron transfer

mechanisms including the reversible and irreversible electron transfer, multi-electron transfer and also the combination or reversible and irreversible steps [47].

Tafel plot

The kinetics of an activation-controlled electrochemical reaction can be described by the Butler-Volmer equation, which is as follows [48]:

$$I = I_0\left[\exp\left(\frac{-\alpha n\eta F}{RT}\right) - \exp\left(\frac{(1-\alpha)n\eta F}{RT}\right)\right] \quad (13)$$

where I_0 is the exchange current density, n is the number of electrons transferred in the reaction, η is the overpotential for the process, α is the symmetry factor, T is the absolute temperature, R is the gas constant and F is the Faraday's constant. Overpotential (η) is the small potential over the equilibrium potential that must be applied to cause an electrodic reaction at a certain rate, mostly in order to overcome the activation barrier for the process. An electrodic reaction may be anodic (oxidation) or cathodic (reduction) depending upon the direction of overpotential with respect to the equilibrium potential of the electrode. The exchange current density (I_0) is the rate at which the charge transfer takes place at the equilibrium potential of the electrode. The lower the exchange current densities slower are the kinetics; hence the larger will be the overpotential. The value of the symmetry factor, α indicates the direction of the electrodic reaction.

At high η, the equation (13) becomes,

$$I = I_0\left[\exp\left(\frac{-\alpha n\eta F}{RT}\right)\right] \quad (14)$$

Taking logarithm on both the sides of equation (14),

$$\eta = \frac{2.303RT}{\alpha nF}\log I_0 - \frac{2.303RT}{\alpha nF}\log I \qquad (15)$$

The equation (15) is known as Tafel equation. The plot of η versus log I is called as the Tafel plot. The Tafel equation can also be written as,

$$\eta = A + B\log I \qquad (16)$$

The slope of the Tafel equation is given by,

$$B = -\frac{2.303RT}{\alpha nF} \qquad (17)$$

At 25 ^{o}C, for n = 1 and α = 0.5, B = -118 mVdec^{-1} (i.e. mV per decade of current).

There are two linear regions which have been identified for the ORR at the Pt electrocatalysts in the alkaline media, ~ 60mVdec^{-1} (α = 1) for a single electron transfer at low overpotentials and 120 mVdec^{-1} (α = 0.5) for a single electron transfer at high overpotentials. They have been interpreted as the change in the rate-determining step from the rapid electron transfer at low overpotentials to a slow electron transfer step at high overpotential.

CHAPTER 2. OXYGEN REDUCTION REACTION ON PLATINUM GOLD ELECTRODES

The PtAu electrodes were first prepared via electrochemical deposition and characterized using cyclic voltammetry and their electrochemically active area was found using copper underpotential deposition. This was followed by the study of their performance towards ORR in the alkaline media using rotating disk electrodes, Koutecky-Levich plots and Tafel plots.

1. Preparation of electrodes

The Pt disk electrode was first polished with 0.03μm alumina. All the electrochemical measurements were performed using the CHI 760 (CH Instruments, Inc.) bipotentiostat.

The solutions of the metals in 0.5M H_2SO_4 were prepared. The solutions were prepared using ultrapure water (resistivity = 18MΩcm). The total concentration of the Pt and Au was maintained at 2 x 10^{-3}M. The metal salts used for electrodeposition were potassium hexachloroplatinate (IV) (K_2PtCl_6) and gold (III) chloride ($AuCl_3$). The molar ratio of Pt:Au was varied as 3:1, 2:1, 1:1, 1:2, 1:3. The electrodes with the Pt:Au ratios of 2:0 and 0:2 were prepared and studied for their performance towards ORR for comparison. The metal solutions were stirred for 3hours before electrodeposition to ensure the dissolution of the metal salts. All the electrode potentials were measured against the Ag/AgCl (3M KCl) reference electrode.

The electrodeposition was carried out under constant stirring by maintaining a constant potential of -0.2V for 10minutes.

2. Electrochemical Characterization

The electrodes were scanned for several times between -0.2V and 1.2V at 100mV/s to clean the electrode. The peaks in the cyclic voltammograms of the electrodes were compared to that of polycrystalline platinum and polycrystalline gold to ensure the purity of the electrode surface. The H_2SO_4 solution was de-oxygenated using high-purity nitrogen for characterization.

The cyclic voltammogram of the electrode with the Pt:Au ratio of 2:0 in nitrogen-purged 0.5M H_2SO_4 is given in figure 2.

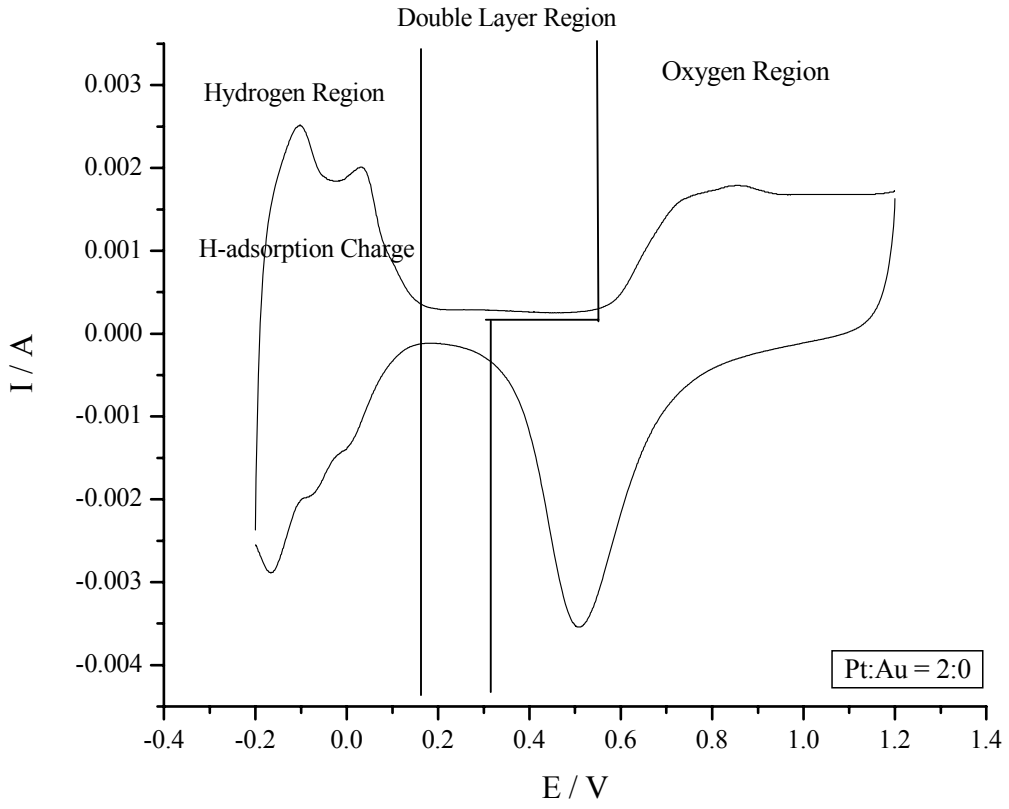

Figure 2: Cyclic voltammogram of a electrode with Pt:Au ratio of 2:0 in N_2 – purged 0.5M H_2SO_4 at a scan rate of 0.1V/s.

The cyclic voltammogram of the electrode with Pt:Au ratio 2:0 matches with the CV of a polycrystalline Pt [49]. The CV shows three distinct regions: hydrogen region, double layer region and the oxygen region. The CV of the electrode deposited with Pt shows H-adsorption region from -0.2V – +0.15V. The theoretical charge for one H-upd is known to be 210μCcm^{-2} for the polycrystalline Pt surface [49].

The cyclic voltammogram of a Pt:Au = 0:2 electrode in is given in the figure 3.

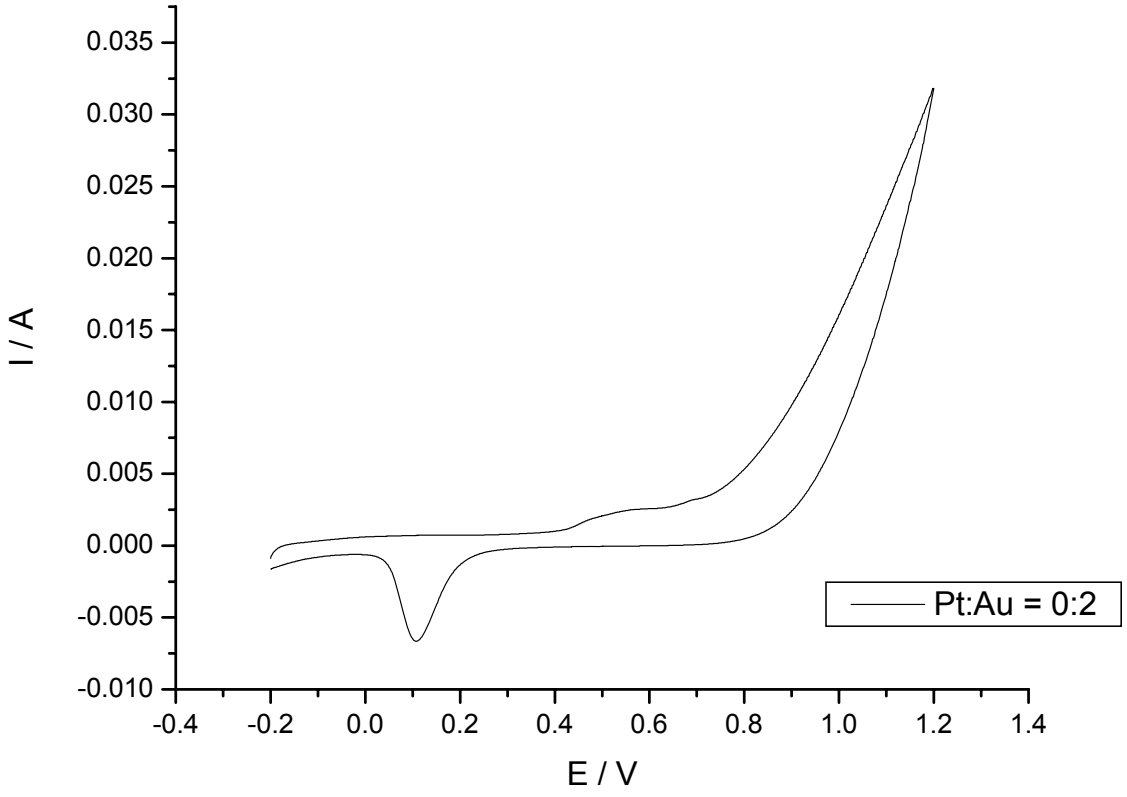

Figure 3: Cyclic voltammogram of Pt:Au = 0:2 electrode in N_2 – purged 0.5M H_2SO_4 at a scan rate of 0.1V/s

The CV of the electrode with Pt:Au ratio of 0:2 electrode showed an oxide reduction peak at 0.1V. The peak was found to shift in the negative direction with respect to the CV of polycrystalline Au [50].

The cyclic voltammograms of the electrodes with the varying Pt:Au ratios is given in figure 4.

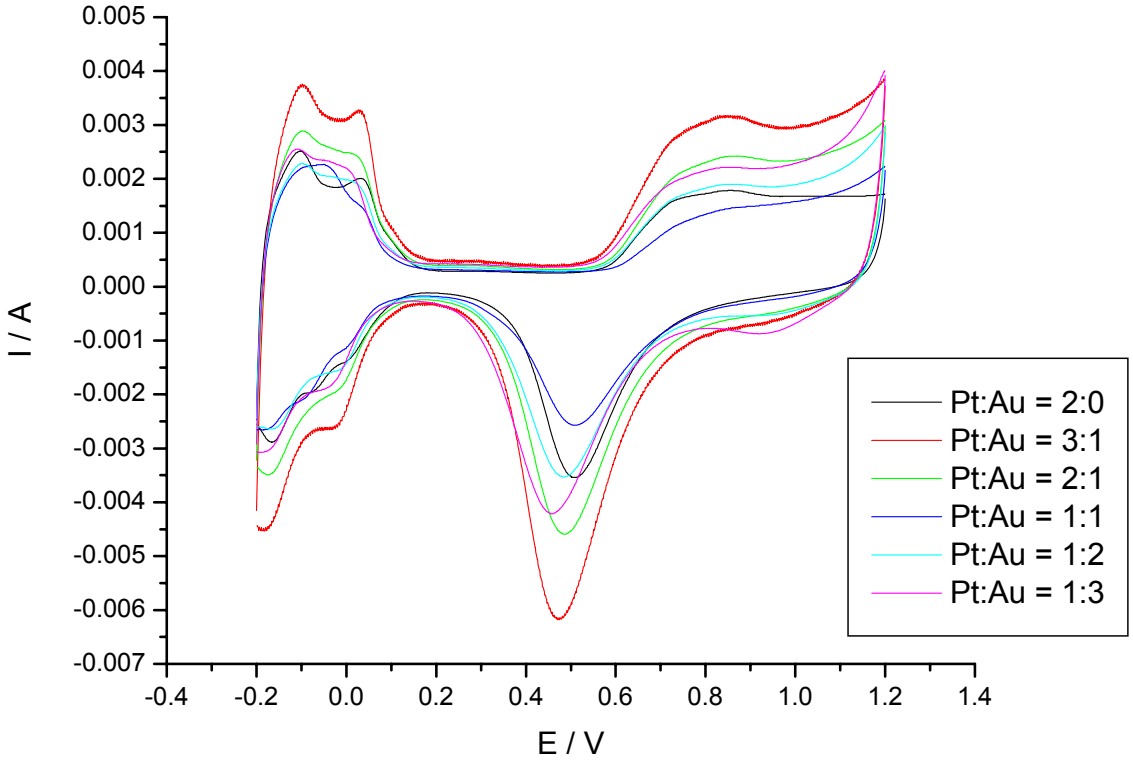

Figure 4: CV of the PtAu electrodes in N_2-purged 0.5M H_2SO_4 at a scan rate of 0.1V/s

The cyclic voltammograms of the PtAu binary electrodes resemble most with the CV of Pt-electrode. The CVs of the electrodes containing the higher content of Pt show larger Pt area from the H-adsorption region. The Pt-area was calculated using the charge under the hydrogen adsorption region of a voltammogram using 210μCcm^{-2} as the conversion factor for charge-to-area. The Pt-area for the various ratios of Pt:Au is given in Table 1.

Table 1: Pt-area of the Pt, PtAu electrodes determined from H-adsorption

Composition of the electrode	Pt-area (H-upd) / cm^2
Pt:Au = 2:0	6.49
Pt:Au = 3:1	8.77
Pt:Au = 2:1	7.29
Pt:Au = 1:1	9.75
Pt:Au = 1:2	5.32
Pt:Au = 1:3	5.38

The Pt-area obtained from the H-adsorption region of the CV decreased with the increase in the content of Au in the catalyst. The Pt-area for Pt:Au electrode with the ratio of 1:1 has been found to be higher than that for 2:1. The irregularities could be attributed to the differences in the speeds of migration of Pt^{4+} and Au^{3+} ions, and to the different morphology observed on the resulting alloys [(7)].

3. Electrochemically active area

The H-adsorption technique limits to the calculation of Pt-area only because of the inability of the H-atoms to adsorb on the Au surface. The copper underpotential deposition (Cu-upd) technique was used to determine the total (Pt and Au) area of the electrode.

The underpotential deposition (upd) is the deposition of the metal atoms onto an electrode surface in mono- or submono- layer quantities at potentials more positive than those required for bulk deposition.

In Cu-upd method, the electrochemically active area of the electrode is covered by a monolayer of Cu. The area of the copper monolayer formed is found by the area of the stripping voltammetry peak of the Cu-monolayer from the electrode. Copper is an ideal metal for upd on both platinum and gold because of the similarity of the atomic radii of the three metals – Cu, 0.128nm; Pt, 0.1385nm; and Au, 0.135nm [51]. The integration of the peak area corresponding to upd stripping allows the surface area to be calculated with the assumption of an adsorption ratio of a single Cu atom to each surface metal atom and an electrosorption valency of +2.

$$Cu_{upd} \rightarrow Cu^{2+} + 2e^{-} \quad Q = 420\mu C cm^{-2} \qquad (18)$$

In our study, the Cu-upd was carried out by biasing a potential of 0.01V vs. Ag/AgCl (3M KCl) through the electrode under study in a 0.005M $CuSO_4$ in 0.1M H_2SO_4. A monolayer of Cu atoms was formed on the electrode surface. The Cu-upd electrodes were scanned in 0.5M H_2SO_4 from -0.2V – 1.2V vs. Ag/AgCl (3M KCl) at the scan rate of 0.1V/s.

The cyclic voltammogram of the Cu-upd Pt:Au ratio 1:1 electrode in 0.5M H_2SO_4 is shown in figure 5.

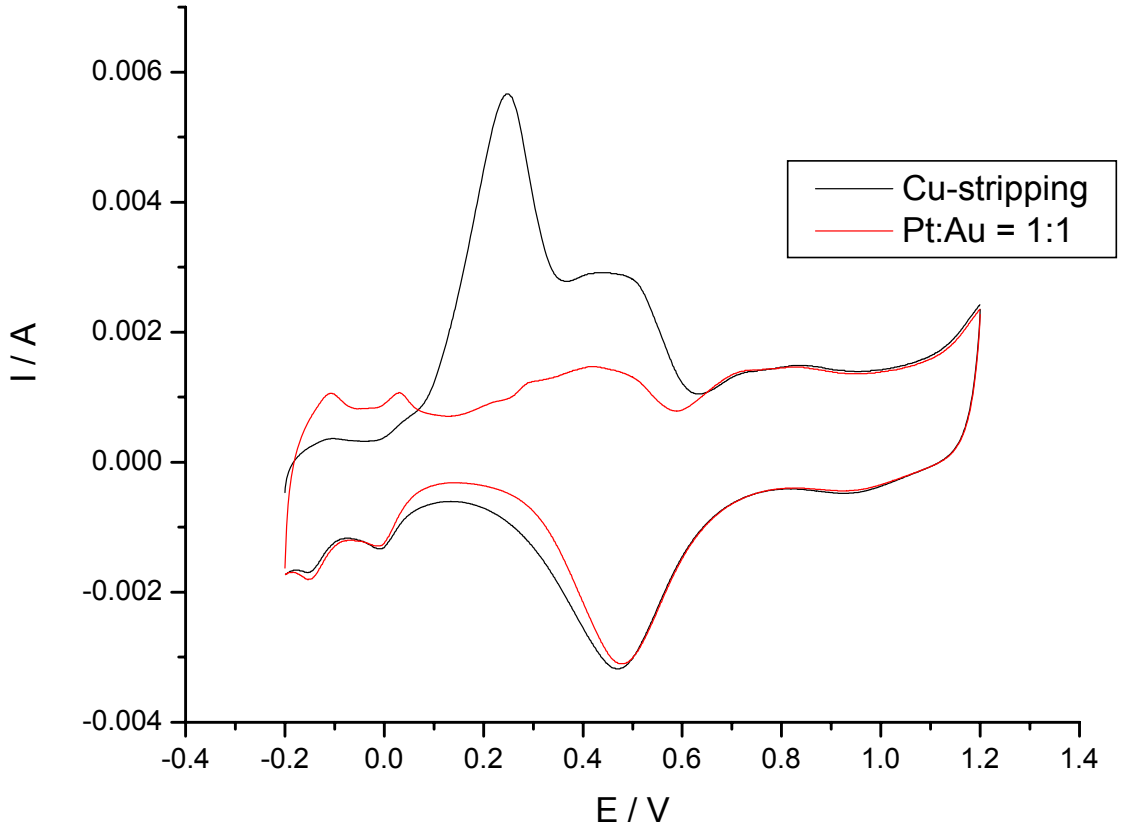

Figure 5: CV of the Cu-upd Pt:Au = 1:1 electrode in N_2 – purged 0.5M H_2SO_4 at a scan rate of 0.1V/s

As shown in figure 5, the ECA was calculated using the charge under the Cu-stripping region of the voltammogram, which is observed in the first oxidation cycle, using 210μCcm^{-2} as the conversion factor for charge-to-area.

The ECA for the electrodes for all the ratios of Pt:Au is given in Table 2.

Table 2: ECA of the Pt, PtAu and Au electrodes from Cu-upd

Composition of the electrode	ECA (Cu-upd) / cm^2
Pt:Au = 2:0	8.37
Pt:Au = 3:1	22.11
Pt:Au = 2:1	6.63
Pt:Au = 1:1	11.27
Pt:Au = 1:2	15.28
Pt:Au = 1:3	9.61
Pt:Au = 0:2	9.53

The ECA of most electrodes were in a good range comparable with each other, except for the electrodes with the Pt:Au ratios 3:1 and 1:2. The total area of the electrodes is the sum of the total atoms of Pt and Au which have formed at the surface. The total atoms of Pt and Au formed at the surface can vary with the differences in the speeds of migration of Pt^{4+} and Au^{3+} ions and their distribution on the surface of the electrode morphology.

The values of ECA for the electrodes were used further in the calculations of kinetic current density, rate constants using Koutecky-Levich plots and Tafel plots.

4. Rotating disk voltammetry

The electrodes were scanned through an anodic sweep from -1.0V to 0.0V at the scan rate of 0.01V/s using the oxygen-saturated 0.1M NaOH as the electrolyte at the rotation speeds from 200rpm – 3600rpm. The NaOH solution was oxygenated with high-purity oxygen for the ORR

studies. The RDE measurements were performed with a modulated speed rotator (Pine Instrument Company). The linear sweep voltammograms of the electrodes at a speed of rotation of 3000rpm with all the Pt:Au ratios is given in figure 6.

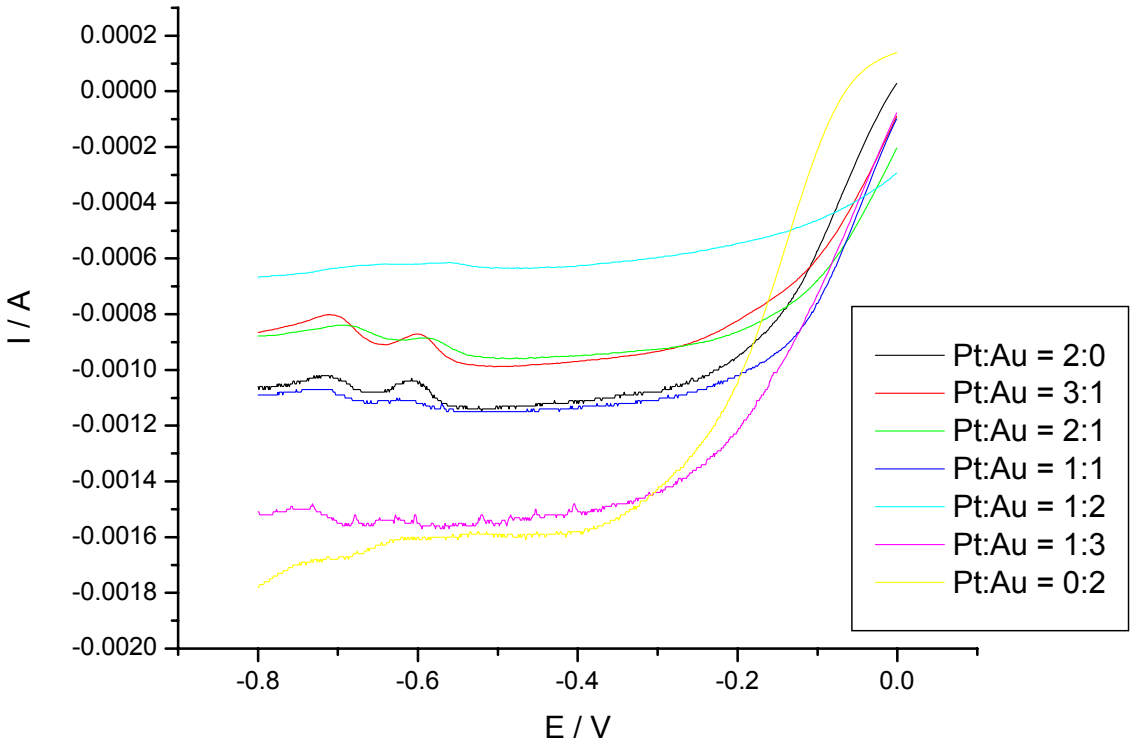

Figure 6: Linear sweep voltammograms of the Pt, PtAu and Au electrodes in 0.1M NaOH at the rotation rate of 3000rpm recoded at the scan rate of 0.01V/s

The linear sweep voltammograms of the electrodes were studied at all speeds of rotation. The electrodes showed a limiting value of the kinetic current density at the rotation rate of 3000rpm. The kinetic current density (i_k) was calculated from the linear sweep voltammograms of the electrodes at -0.4V.The i_k values for the electrodes at 3000rpm are given in Table 3.

Table 3: Kinetic current densities of the Pt, PtAu and Au electrodes from RDE in oxygen-saturated 0.1M NaOH at 3000rpm

Composition of the electrode	i_k at -0.4V / μAcm^{-2}
Pt:Au = 2:0	132
Pt:Au = 3:1	43
Pt:Au = 2:1	141
Pt:Au = 1:1	100
Pt:Au = 1:2	40
Pt:Au = 1:3	156
Pt:Au = 0:2	164

The values of the kinetic current density have been found to increase with the increase in the amount of Au added to the electrode.

5. Koutecky-Levich Plots

The limiting current density for all the electrodes were found from the linear sweep voltammograms obtained for every rotation speed. The Koutecky-Levich plots, (I^{-1} vs. $\omega^{-1/2}$) were plotted using the MS Excel program.

The Koutecky-Levich plot for the electrode with the Pt:Au ratio 2:0 is shown in figure 7.

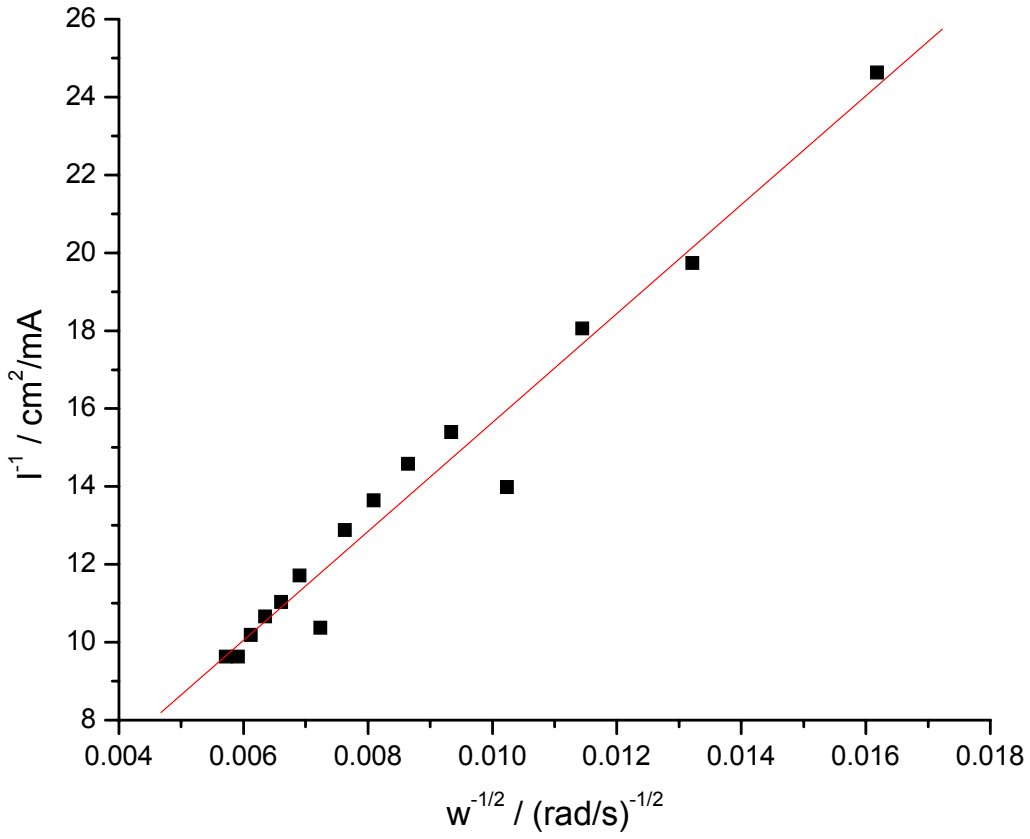

Figure 7: Koutecky-Levich plot for the Pt:Au = 2:0 electrode

The Koutecky-Levich plots of the electrodes towards ORR show a linear relationship between I^{-1} and $\omega^{-1/2}$. This indicates the first order kinetics for the oxygen reduction reaction on the electrodes.

The values of the intercepts of the Koutecky-Levich plots were used to calculate the rate constants of the electron transfer reaction. From the Koutecky-Levich equation (equation 13), the intercept equals to $1/nFk_fC$. The value of n = 4 (overall four-electron transfer reaction), F is the Faraday's constant (F = 96,485Cmol^{-1}), C is the solubility of oxygen in the sodium hydroxide solution at 25^{o}C (c = 1.2 x 10^{-6}molcm^{-3}) [52].

The values of the rate constants obtained from the Koutecky-Levich equation for the various compositions of the electrode is given in Table 4.

Table 4: Rate constants for the ORR for all the ratios of Pt, Au calculated from the Koutecky-Levich plots

Composition of the electrode	Rate constant, k_f / cms^{-1}
Pt:Au = 2:0	$2.44x10^{-3}$
Pt:Au = 3:1	$8.27x10^{-3}$
Pt:Au = 2:1	$1.53x10^{-2}$
Pt:Au = 1:1	$5.74x10^{-3}$
Pt:Au = 1:2	$5.38x10^{-2}$
Pt:Au = 1:3	$1.26x10^{-3}$
Pt:Au = 0:2	$5.55x10^{-3}$

The values of the rate constants increased from Pt:Au ratio 2:0 with an increasing content of Au till the Pt:Au ratio 1:2. The value of the rate constant was lower in the electrode with Pt:Au ratio 1:3 and was low for the Pt:Au ratio = 0:2. This indicates that the rate constants for ORR increase with the addition of small amounts of Au in the electrode.

6. Tafel plots

The Tafel plots, i.e. E (V) vs log$I(Acm^{-2})$, were plotted for the electrodes with all Pt:Au ratios. The Tafel plots for the electrodes are given in figure 8.

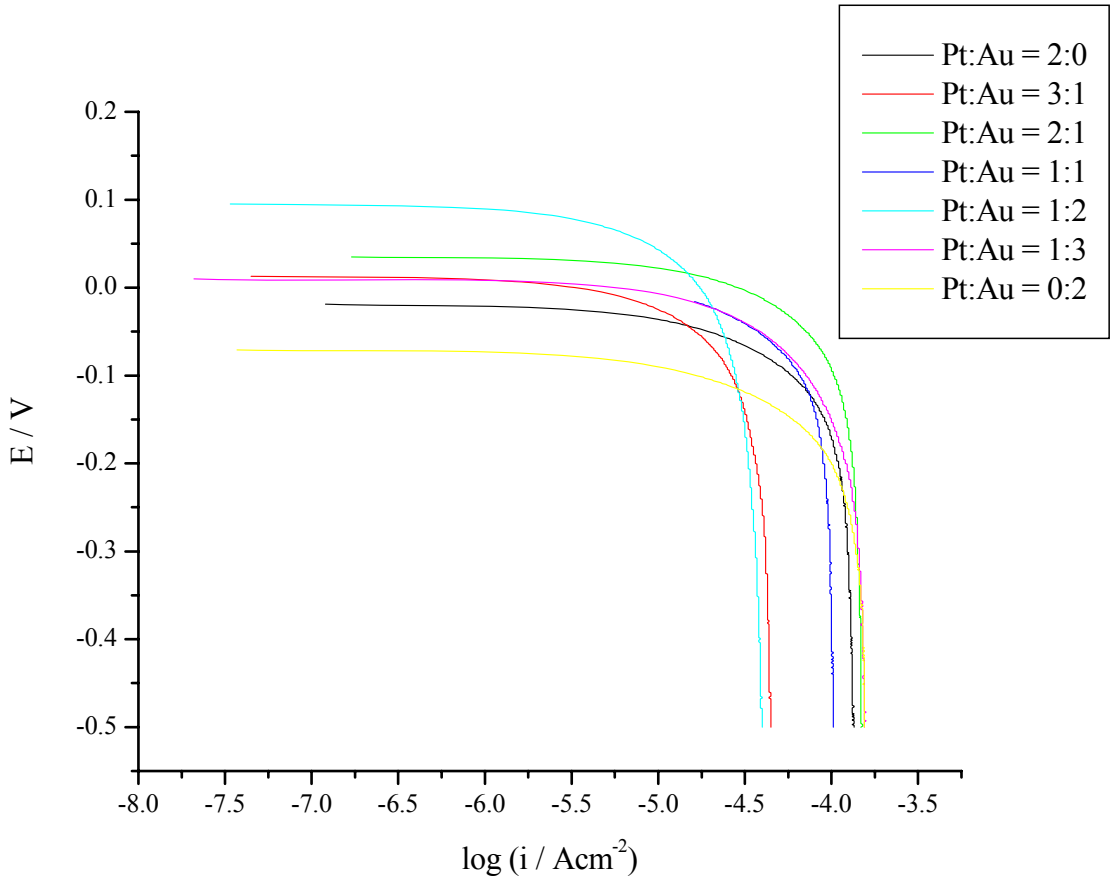

Figure 8: Tafel plots for the ORR on the electrodes with all the Pt:Au ratios in 0.1M NaOH plotted at a scan rate of 0.01V/s

The Tafel plots for all the electrodes show two distinct regions for the two electron transfer processes, a steadily changing low current density region and an extremely steep high current density region. The slopes of the curves were calculated in both the region using MS Excel program.

The values of the Tafel slopes obtained for the various compositions of the electrodes are given in Table 5.

Table 5: Tafel slopes in the low and high current density region of the Tafel plots for the PtAu electrodes towards ORR at 3000rpm

Composition of the electrode	Tafel slope at low current density / $mVdec^{-1}$	Tafel slope at high current density / $mVdec^{-1}$
Pt:Au = 2:0	91	467
Pt:Au = 3:1	83	452
Pt:Au = 2:1	97	528
Pt:Au = 1:1	182	399
Pt:Au = 1:2	105	478
Pt:Au = 1:3	138	530
Pt:Au = 0:2	99	403

The Tafel slopes in the low current density region have lower values (~$90mVdec^{-1}$) which indicate higher rates for the first electron transfer. The values of Tafel slopes increased with the increase in the Au content which indicates that the rates were higher for the small Au content in the electrodes. The Tafel slopes in the high current density region have very high values which indicate lower rates for the second electron transfer.

CHAPTER 3. OXYGEN REDUCTION REACTION ON NANOCERIA-MODIFIED PLATINUM GOLD ELECTRODES

The nanoceria modified PtAu (PtAu/CeO2) electrodes were prepared, characterized and their electrochemically active area was determined. Their performance towards ORR in the alkaline media was studied and the results were compared with those of the PtAu electrodes.

1. Preparation of electrodes

The total concentration of the Pt and Au was maintained at 2 x 10^{-3}M. The molar ratio of Pt:Au was varied as 3:1, 2:1, 1:1, 1:2, 1:3. The concentration of nanoceria was maintained at 5 x 10^{-3}M. The electrodes with the Pt:Au ratios 2:0 and 0:2 were prepared and studied for their performance towards ORR for comparison. The solutions were stirred for 3hours before electrodeposition to ensure the dissolution of the metal salts and uniform dispersion of nanoceria in the solution. The electrodeposition was carried out under constant stirring of -0.2V for 10minutes. The rate of stirring was maintained constant for all the ratios of Pt and Au.

2. Electrochemical Characterization

The electrode was scanned for several times between -0.2V and 1.2V at 100mV/s to clean the electrode. The electrochemical response of the working electrode was examined in N_2-saturated 0.5M H_2SO_4 versus Ag/AgCl, 3M KCl electrode. The cyclic voltammograms for the ceria-modified electrodes along with the unmodified electrodes is given in figure 9.

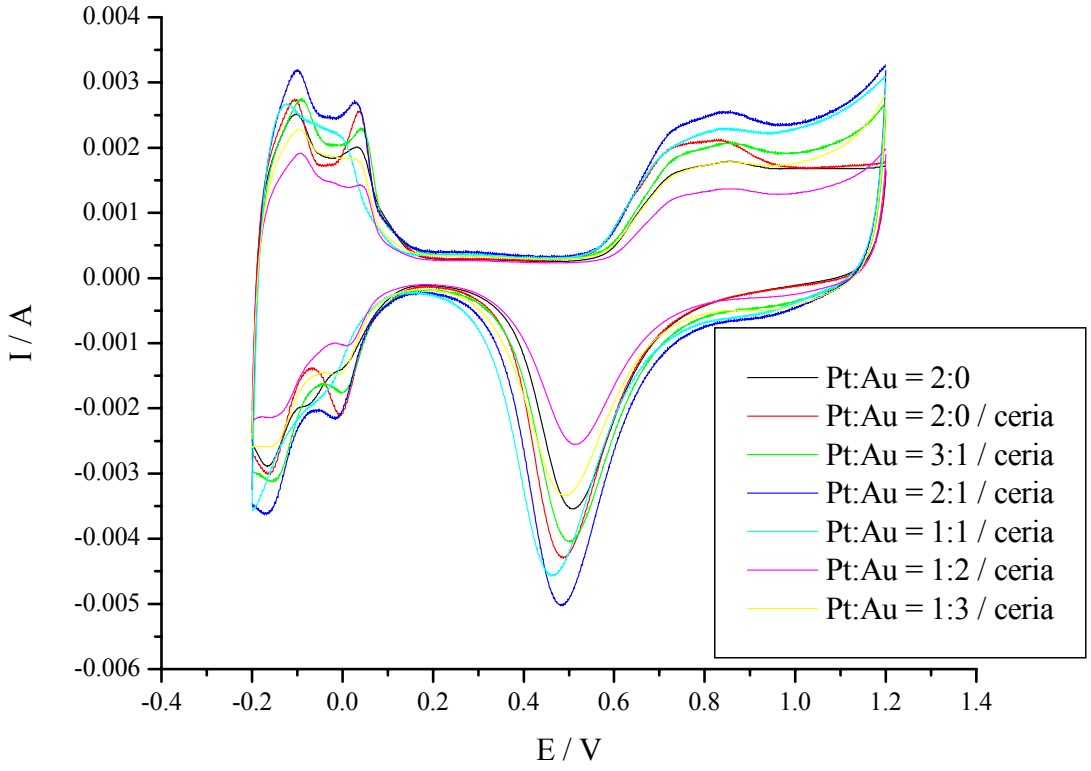

Figure 9: CV of the Pt, ceria-modified Pt, ceria-modified PtAu and Au electrodes in N_2 – purged 0.5M H_2SO_4 at a scan rate of 0.1V/s

The cyclic voltammograms of the ceria-modified electrodes were close to that of the Pt electrode. The Pt-area of the electrodes was calculated using the charge under the hydrogen adsorption region of the voltammograms using 210μCcm^{-2} as the conversion factor for charge-to-area. The Pt-area for the electrodes with all the ratios of Pt:Au is given in Table 6.

Table 6: Pt-area of the electrodes with all the ratios of Pt, Au and ceria modified PtAu determined from H-upd

Composition of the electrode	Pt-area (H-upd) / cm^2
Pt:Au = 2:0	6.49
Pt:Au = 2:0 / ceria	6.66
Pt:Au = 3:1 / ceria	7.31
Pt:Au = 2:1 / ceria	7.75
Pt:Au = 1:1 / ceria	4.71
Pt:Au = 1:3 / ceria	5.85
Pt:Au = 1:2 / ceria	5.14

There was an overall increase in the Pt-area of the ceria-modified electrodes as compared with that of the unmodified electrodes. The Pt-area of the electrodes decreases with the increase in the content of Au in the catalyst.

3. Electrochemically active area

The electrochemically active area (ECA) of the electrodes was found out using the Cu-upd. The ECA was calulated using the charge under the copper stripping region of a voltammogram of Cu-underpotential deposited electrode in 0.5M H_2SO_4 using 420μCcm^{-2} as the conversion factor for charge-to-area.

The upd of copper was carried out by passing a potential of 0.01V vs. Ag/AgCl (3M KCl) through the electrode under study in a 0.005M $CuSO_4$ in 0.1M H_2SO_4. A monolayer of Cu atoms was formed on the electrode surface. The Cu-upd electrode was scanned in 0.5M H_2SO_4 from -

0.2V – 1.2V vs. Ag/AgCl at the scan rate of 0.1V/s. The CV of the Cu-upd nanoceria-modified Pt:Au ratio 1:1 ratio is given in figure 10.

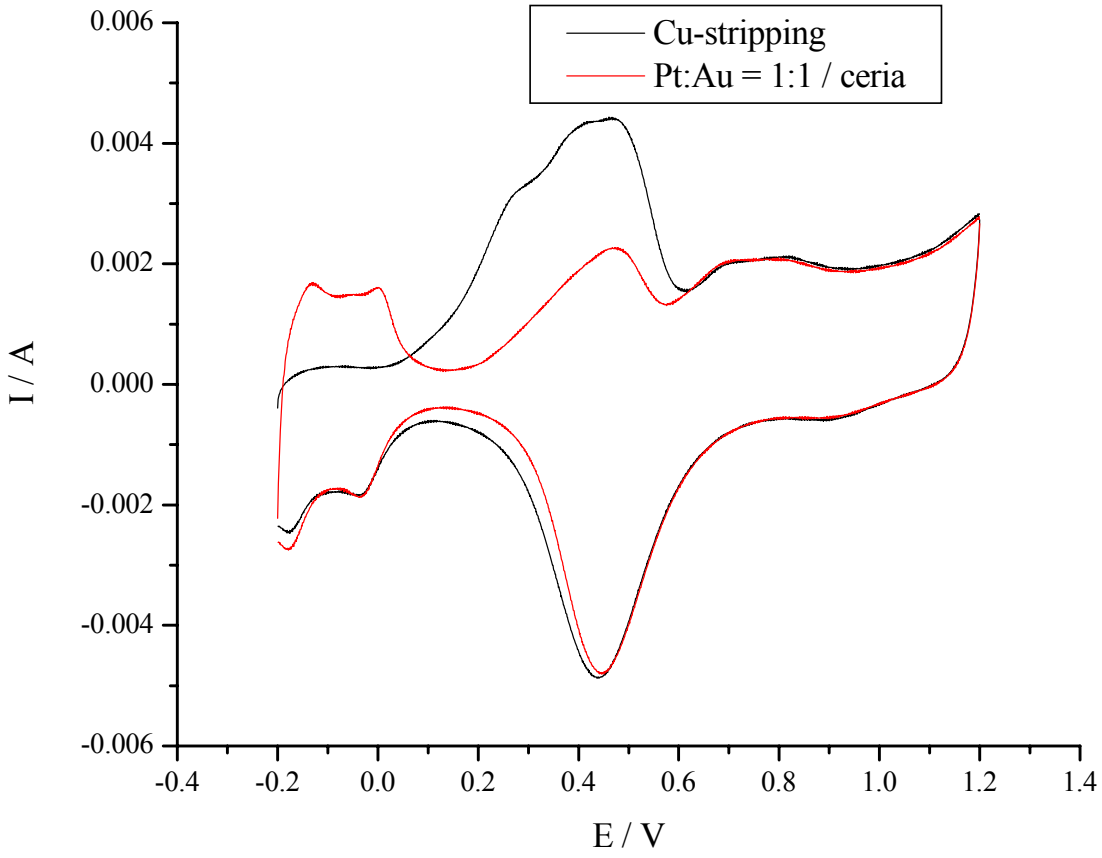

Figure 10: CV of the Cu-upd Pt:Au = 1:1 / ceria electrode in N_2 – purged 0.5M H_2SO_4 at a scan rate of 0.1V/s

The copper stripping peak is seen in the first oxidation cycle of the CV. The ECA for the electrodes with all the Pt:Au ratios are given in Table 7.

Table 7: ECA of the Pt, Au and PtAu/CeO_2 determined from Cu-upd

Composition of the electrode	ECA (Cu-upd) / cm^2
Pt:Au = 2:0	8.37
Pt:Au = 2:0 / ceria	12.02
Pt:Au = 3:1 / ceria	10.26
Pt:Au = 2:1 / ceria	14.76
Pt:Au = 1:1 / ceria	13.93
Pt:Au = 1:3 / ceria	11.85
Pt:Au = 1:2 / ceria	14.49
Pt:Au = 0:2	9.53

The values of ECA were in a good range for all the ratios of Pt:Au in the electrodes. The ECA of the ceria-modified electrodes was larger than that of the unmodified electrodes with all ratios of Pt:Au due to the increased porosity which is imparted by ceria.

The values of ECA for the electrodes were used further in the calculations of kinetic current density, rate constants using Koutecky-Levich plots and Tafel plots.

4. Rotating disk electrodes

The electrodes were scanned through an anodic sweep from -1.0V to 0.0V at the scan rate of 0.01V/s using the oxygen-saturated 0.1M NaOH as the electrolyte at the rotation speeds from 200rpm – 3600rpm. The NaOH solution was oxygenated with high-purity oxygen for the ORR studies. The linear sweep voltammograms of the ceria-modified electrodes at 3000rpm with all the Pt:Au ratios are given in figure 11.

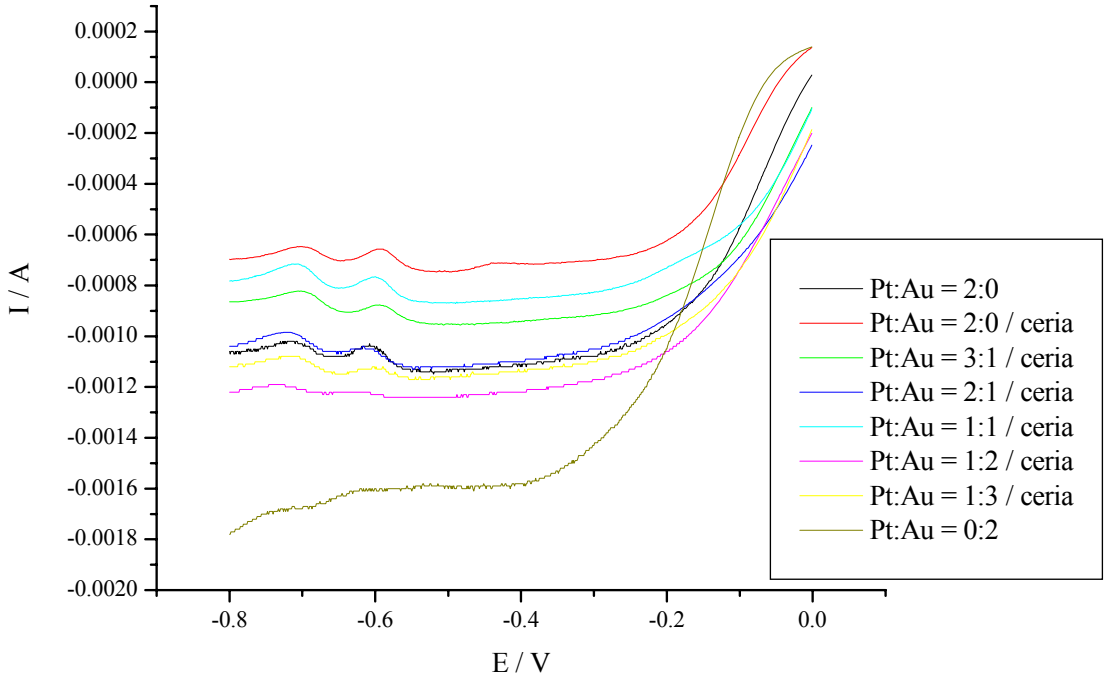

Figure 11: Linear sweep voltammograms of the Pt, ceria-modified PtAu and Au electrodes in 0.1M NaOH at the rotation rate of 3000rpm recoded at the scan rate of 0.01V/s

The linear sweep voltammograms of the electrodes were studied at all speeds of rotation. The electrodes showed a limiting value of the kinetic current density at the rotation rate of 3000rpm. The kinetic current density (i_k) was calculated from the linear sweep voltammograms of the electrodes at -0.4V.The i_k values for the electrodes at 3000rpm are given in Table 8.

Table 8: Kinetic current densities of the Pt, PtAu/CeO_2 and Au electrodes from RDE in oxygen-saturated 0.1M NaOH at 3000rpm

Composition of the electrode	i_k at -0.4V / μAcm^{-2}
Pt:Au = 2:0	132
Pt:Au = 2:0 / ceria	59
Pt:Au = 3:1 / ceria	91
Pt:Au = 2:1 / ceria	73
Pt:Au = 1:1 / ceria	61
Pt:Au = 1:2 / ceria	102
Pt:Au = 1:3 / ceria	77
Pt:Au = 0:2	164

The values of the kinetic current density have been found to increase with the increase in the amount of Au added to the electrode. This indicates the increase in the ORR rate with the increase of Au in the electrodes. The values of i_k for the nanoceria-modified PtAu electrodes are lower than those of the unmodified electrodes due to the lower electrical conductivity of ceria.

5. Koutecky-Levich plots

The limiting current density for all the electrodes were found from the linear sweep voltammograms obtained for every rotation speed. The Koutecky-Levich plots (I^{-1} vs. $\omega^{-1/2}$) were

plotted using the MS Excel program. The Koutecky-Levich plot for the Pt:Au = 2:0 / ceria electrode is given in figure 11.

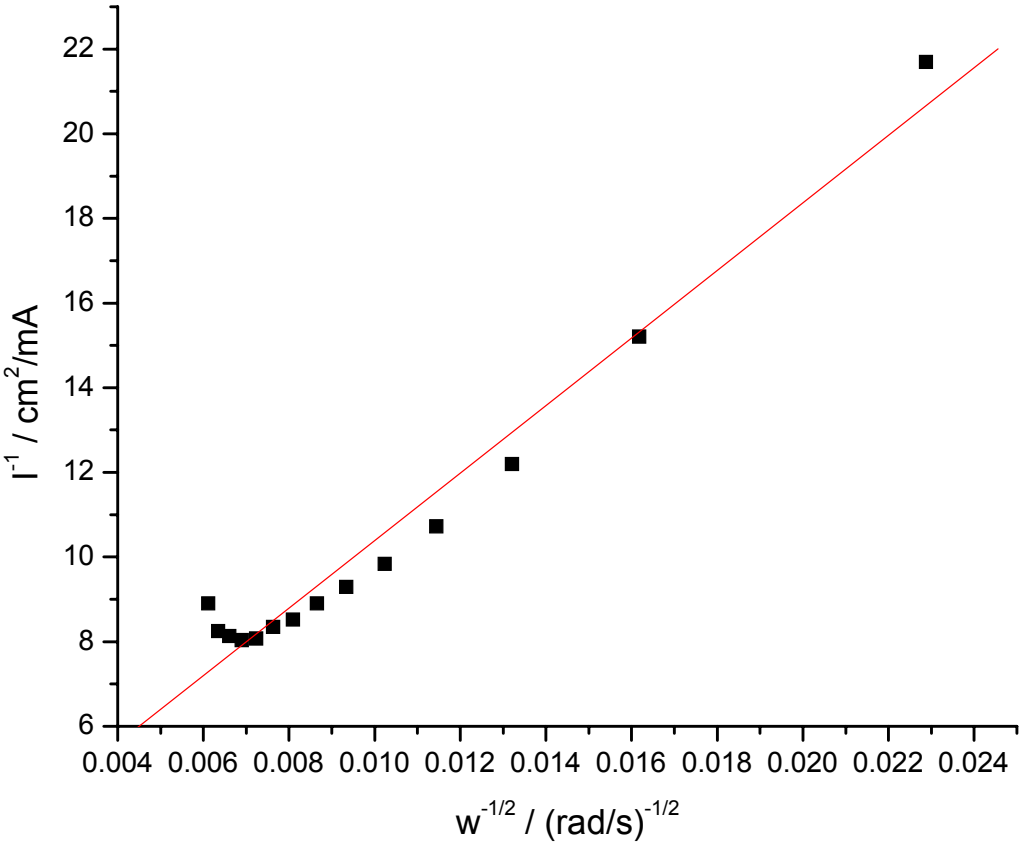

Figure 12: Koutecky-Levich plot for the Pt:Au = 2:0 / ceria electrode

The Koutecky-Levich plots of the electrodes towards ORR show a linear relationship between I^{-1} and $\omega^{-1/2}$. This indicates the first order kinetics for the oxygen reduction reaction on the ceria-modified electrodes also.

The values of the rate constants obtained from the Koutecky-Levich equation for the various compositions of the electrodes is given in table 9.

Table 9: Rate constants for the ORR for all the ratios of Pt, Au and ceria-modified PtAu calculated from the Koutecky-Levich plots

Composition of the electrode	Rate constant (k_f) / cms^{-1}
Pt:Au = 2:0	$2.44x10^{-3}$
Pt:Au = 2:0 / ceria	$2.02x10^{-3}$
Pt:Au = 3:1 / ceria	$1.73x10^{-2}$
Pt:Au = 2:1 / ceria	$2.36x10^{-3}$
Pt:Au = 1:1 / ceria	$2.08x10^{-3}$
Pt:Au = 1:2 / ceria	$3.66x10^{-2}$
Pt:Au = 1:3 / ceria	$1.66x10^{-2}$
Pt:Au = 0:2	$5.55x10^{-3}$

The values of the rate constants obtained using ceria-modified electrodes increased with an increasing content of Au. The values of the rate constants for the ceria-modified electrodes were of the comparable orders as the unmodified electrodes.

6. Tafel plots

The Tafel plots, i.e. E (V) vs log$I(Acm^{-2})$ were plotted for the nanoceria-modified electrodes with varying Pt:Au ratios. The Tafel plots for the electrodes with all the Pt:Au ratios are given in figure 13.

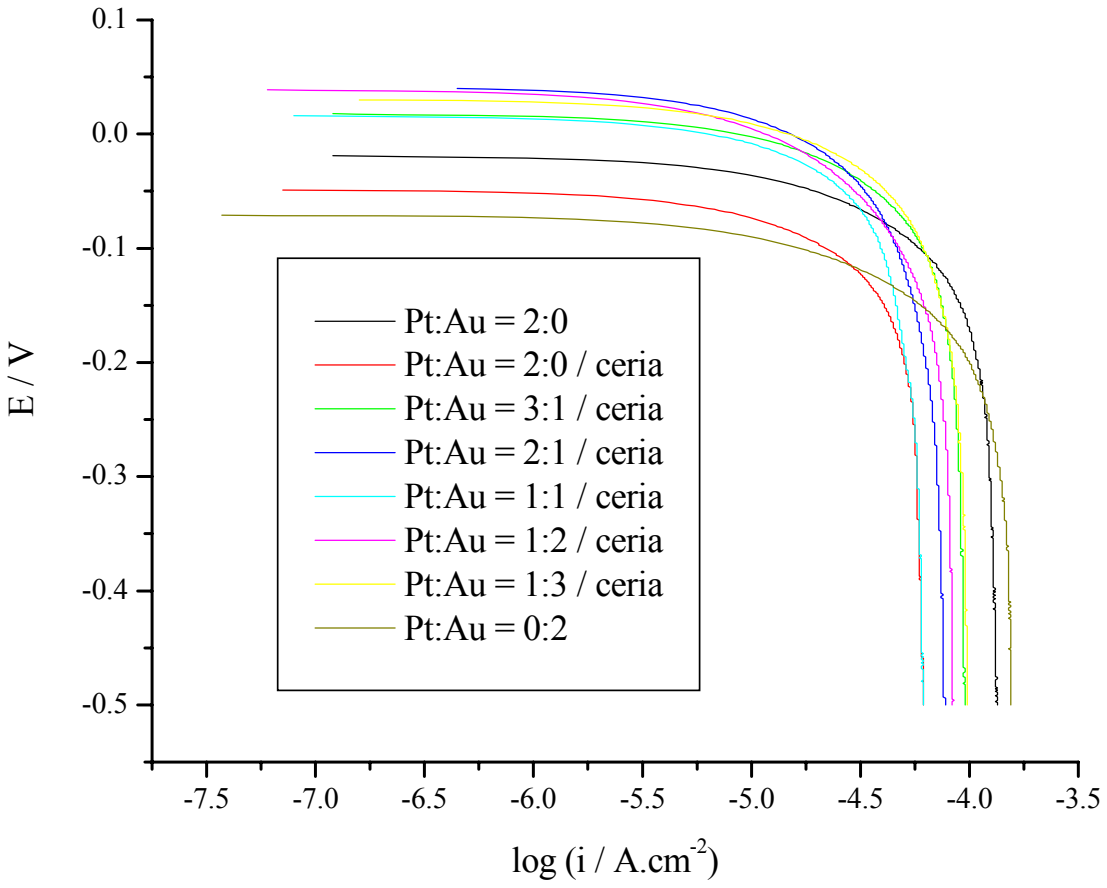

Figure 13: Tafel plots for the electrodes with the Pt, ceria-modified PtAu and Au electrodes in 0.1M NaOH plotted at a scan rate of 0.01V/s

The Tafel plots obtained for the ceria-modified electrodes were almost similar in nature to the unmodified electrodes. The Tafel plots for the ceria-modified electrodes show two distinct regions for the two electron transfer processes, a steadily changing low current density region and an extremely steep high current density region. The slopes of the curves were calculated in both the region using MS Excel program.

The values of the Tafel slopes obtained for the various compositions of the electrodes are given in Table 10.

Table 10: Tafel slopes in the low and high current density region of the Tafel plots for the PtAu/CeO_2 electrodes towards ORR at 3000rpm

Composition of the electrode	Tafel slope at low current density / $mVdec^{-1}$	Tafel slope at high current density / $mVdec^{-1}$
Pt:Au = 2:0	91	467
Pt:Au = 2:0 / ceria	129	441
Pt:Au = 3:1 / ceria	188	393
Pt:Au = 2:1 / ceria	208	423
Pt:Au = 1:1 / ceria	133	563
Pt:Au = 1:2 / ceria	198	288
Pt:Au = 1:3 / ceria	212	357
Pt:Au = 0 :2	123	403

The Tafel slopes in the low current density region have higher values (~180$mVdec^{-1}$) which indicate comparatively lower rates for the first electron transfer. The values of Tafel slopes increased with the increase in the Au content which indicates that the rates were higher for the small Au content in the electrodes. The Tafel slopes in the high current density region have very high values which indicate lower rates for the second electron transfer.

CHAPTER 4. CONCLUSION

1. Performance of PtAu and PtAu/CeO2 towards ORR

The performance of the PtAu and PtAu/CeO_2 catalysts towards the ORR was studied. The catalytic activity due to the addition of Au in Pt was studied. Also, the effect of incorporating ceria in the PtAu alloy was studied. The values of the kinetic-controlled current density were obtained for both the PtAu and PtAu/CeO_2 electrodes from the RDE voltammetry in 0.1M NaOH at -0.4V at a rotation speed of 3000rpm. The kinetic current density was found to increase with an increase in the content of Au in the PtAu electrodes. This indicated that the rate of ORR increased with the increase in the content of Au in the electrode. The values of the kinetic current density were lower for the PtAu/CeO_2 electrodes as compared to the PtAu electrodes. This indicated the lower rates of the ORR on the PtAu/CeO_2 electrodes. This can also be attributed to the lower electrical conductivity of ceria. The Koutecky-Levich plots (I^{-1} vs. $\omega^{-1/2}$) for the PtAu electrodes and the PtAu/CeO_2 were straight line plots for the value of n = 4 (number of electrons transferred) for ORR. This indicated the first order kinetics for both the PtAu and PtAu/CeO_2 electrodes towards the four-electron transfer process of ORR. The values of the rate constants obtained from the Koutecky-Levich plots were found to increase with the addition of small amounts of Au in the electrode and were found to decrease with the addition of higher amounts of Au. The values of the ORR rate constants for the PtAu/CeO_2 electrode were of the comparable order of magnitudes to that for the PtAu electrodes.

The values of Tafel slopes for the PtAu electrodes in the low current density region of the Tafel plot were lower (~90mVdec^{-1}) which indicates higher rates of electron transfer. The Tafel slopes

increased with the larger amounts of Au which indicates that the rates of electron transfer were reduced with the addition of larger amounts of Au in the electrode. The values of Tafel slopes for the PtAu electrodes were very high in the high current density region which indicates the low rates for the electron transfer process in the high current density region. The values of Tafel slopes for the PtAu/CeO_2 electrodes were high in both the low and high current density region which indicates lower rates of electron transfer for the PtAu/CeO_2 electrodes. The lower rates of electron transfer in the PtAu/CeO_2 electrodes can be attributed to the lower electrical conductivity of ceria. The lower rates indicate the higher rates of formation of the stable oxygen species, or the conversion of the hydroperoxide anion back into water and oxygen. The lower rates of ORR on PtAu/CeO_2 electrodes can also be attributed to the formation of the Pt-oxide layer which controls the adsorption of oxygen on the Pt surface thus affecting the rate of first electron transfer in the process of the reduction of oxygen.

From the results obtained, we can conclude that the addition of Au in small amounts to Pt in the electrodes prepared via electrodeposition enhances the catalytic ability of Pt catalyst towards the kinetics of oxygen reduction reaction. The modification of the PtAu catalyst with nanoceria however reduces the catalytic ability of the PtAu catalyst mainly due to its poor electrical conductivity though the addition of ceria actually increases the surface area of the catalyst.

2. Path forward

The contribution of ceria towards the catalytic ability of the PtAu catalyst needs to be studied. The variation in the concentration of ceria, maintaining the total concentration of Pt and Au constant, will allow the study of contribution of oxygen releasing effect vs. electrical conductivity of ceria towards ORR catalysis in a qualitative and quantitative manner. The RRDE

study of the ORR by the PtAu/CeO_2 composite needs to be studied since it helps in understanding the mechanism of ORR in much more detail. The presence of the Pt ring in conjunction with the disk will allow the detection of H_2O_2 and other active oxygen species formed in the ORR process and also allow studying the role the species contribute to the performance of the catalyst towards ORR kinetics.

The incorporation of metal oxides with a lower bandgap, such as TiO_2 [53] for example, into the PtAu catalyst can contribute towards higher rates of electron transfer and enhance the rates of ORR. The incorporation of chalcogenides with a lower bandgap can also contribute towards higher rates of electron transfer and enhance the rates of ORR. The incorporation of conductive polymer materials such as polyaniline, for example, can also increase the rates of electron transfer [54, 55] through the electron-hole hoping mechanism and increased porosity in their networks and enhance the rates of ORR. The addition of polyaniline has shown to exhibit improved methanol tolerance in a direct methanol fuel cell [56].

REFERENCES

1. Carrette, L., Friedrich, K., Stimming, U., *Fuel Cells*, **2001**, 1, 5.

2. Halpert, G., Frank, H., Surampudi, S., *The Electrochem. Soc. INTERFACE*, **1999**, 8, 25.

3. Larminie, J., Dicks, A., *Fuel Cell Systems Explained*, John Wiley & Sons, England, 2nd Ed., **2003**.

4. Markovic, N., Grgur, B., Ross, P., *J. Phys. Chem. B*, **1997**, 101, 5405.

5. Bai, L., Harrington, P., Conway, B., *Electrochim. Acta*, **1987**, 32, 1713.

6. Atanassova, P., et al, *Proc. ECS Meeting*, **2001**, San Francisco, Abs. 333.

7. Anderson, J., Karakoti, A., Diaz, D., Seal, S., *J. Phys. Chem. C*, **2010**, 114, 4595.

8. Kinoshita, K., *Electrochemical Oxygen Technology*, Wiley, New York, **1992**.

9. Markovic, N., Schmidt, T., Stamenkovic, V., Ross, P., *Fuel Cells*, **2005**, 1, 105.

10. Spendelow, J., Wieckowski, A., *Phys. Chem. Chem. Phys.*, **2007**, 9, 2654.

11. Gasteiger, H., Kocha, S., Sompalli, B., Wagner, F., *Appl. Catal. B: Environ.*, **2005**, 56, 9.

12. Salgado, J., Antolini, E., Gonzalez, E., *Appl. Catal. B: Environ.*, **2005**, 57, 283.

13. Lima, F., Salgado, J., Gonzalez, E., Ticianelli, E., *J. Electrochem. Soc.*, **2007**, 154, A369.

14. Mukerjee, S., Srinivasan, S., Soriaga, M., *J. Phys. Chem.*, **1995**, 99, 4577.

15. Stamenkovic, V., Schmidt, T., Ross, P., Markovic, N., *J. Phys. Chem. B*, **2002**, 106, 11970.

16. Lim, D., Lee, W., Choi, D., Kwon, H., Lee, H., *Electrochem. Commun.*, **2008**, 10, 592.

17. Lee, K., Kwon, K., Roev, V., Yoo, D., Chang, H., Seung, D., *J. Power Sources*, **2008**, 185, 871.

18. Liu, Y., Ishihara, A., Mitsushima, S., Kamiya, N., Ota, K., *Electrochem. Solid-State Lett.*, **2005**, 8, A400.

19. Lim, D., Lee, W., Macy, N., Smyrl, W., *Electrochem. Solid-State Lett.*, **2009**, 12, B123.

20. Yu, H., Kim, J., Lee, H., Schibioh, M., Lee, J., Han, J., Yoon, S., Ha, H., *J. Power Sources*, **2005**, 140, 59.

21. E. Antolini, E., Gonzalez, E., *Solid State Ionics*, **2009**, 180, 746.

22. Kuwaha, K., Matsuoka, A., *Japan Patent*, **1998**, 10-55807.

23. Xu, Z., Qi, Z., Kaufman, A., *J. Power Sources*, **2003**, 115, 40.

24. Trovarelli, A., *Catalysis by Ceria and Related Materials*, Imperial College Press, London, U.K., **2002**.

25. Diaz, D., Greenletch, N., Solanki, A., Karakoti, A., Seal, S., *Catal. Lett.*, **2007**, 119, 319.

26. Jiang, L., Hsu, A., Chu, D., Chen, R., *J. Electrochem. Soc.*, **2009**, 156, B370.

27. Lim, D., Lee, W., Choi, D., Lee, H., *Appl. Catal. B. Envir.*, **2010**, 94, 85.

28. Adzic, R., in: Lipkowski, J., Ross, P. (Eds), *Electrocatalysis*, Wiley-VCH, New York, **1998**, p. 197.

29. Markovic, N., Schmidt, T., Stamenkovic, V., Ross, P., *Fuel Cells*, **2005**, 1, 105.

30. Markovic, N., Ross, P., in: Wieckowski, A. (Ed.), *Interfacial Electrochemistry – Theory, Experiments and Applications*, Marcel Dekker, New York, **1999**, p. 821.

31. Hsueh, K., Gonzalez, E., Srinivasan, S., *Electrochim. Acta*, **1983**, 28, 691.

32. Lipp, L., Gottesfeld, S., Chlistunoff, J., *J. Appl. Electrochem.*, **2005**, 35, 1015.

33. Furuya, N., Aikawa, H., *Electrochim. Acta*, **2000**, 45, 4251.

34. Carlsson, L., Ojefors, L., *J. Electrochem. Soc.*, **1980**, 127, 525.

35. Yang, C., *Int. J. Hydrogen Energ.*, **2004**, 29, 135.

36. Gervasio, D., Payer, J., *Proc. Electrochem. Soc.*, **2005**, P2003-30, 58.

37. Vago, E., Calvo, E., *J. Electroanal. Chem.*, **1992**, 339, 41.

38. Wroblowa, H., Qaderi, S., *J. Electroanal. Chem. Interfacial Electrochemi.*, **1990**, 295, 153.

39. Yeager, E., *Electrochim. Acta*, **1984**, 29, 1527-1537.

40. Schmidt, T., Stamenkovic, V., Arenz, M., Markovic, N., Ross, P., *Electrochim. Acta*, **2002**, 47, 3765.

41. Tacconi, N., Rajeshwar, K., Chanmanee, W., Valluri, V., Wampler, W., Lin, W., Nikiel, L., *J. Electrochem. Soc.*, **2010**, 157, B147.

42. Guo, S., Dong, S., Wang, E., *J. Phys. Chem. C*, **2009**, 113, 5485.

43. Kristian, N., Wang, X., *Electrochem. Commun.*, **2008**, 10, 12.

44. Liu, C., Wei, Y., Wang, K., *Chem. Commun.*, **2010**, 46, 2483.

45. Liu, C., Wei, Y., Wang, K., *Electrochem. Commun.*, **2009**, 11, 1362.

46. Brett, C., Brett, A., *Electrochemistry: Principles, Methods and Applications*, Oxford, University Press Inc., N.Y., **1993**.

47. Treimer, S., Tang, A., Johnson, D., *Electroanal.*, **2002**, 14, 165.

48. Bard, A., Faulkner, L. *Electrochemical Methods: Fundamentals and Applications*, John Wiley & Sons, New York, 2nd Edition, **2000**.

49. Rodríguez, J., Melian, J., Pena, J., *J. Chem. Ed.*, **2000**, 77, 1195.

50. Merrill, D., Stefan I., Scherson, D., Mortimer, J., *J. Electrochem. Soc.*, **2005**, 152, E212.

51. Green, C., Kucernak, A., *J. Phys. Chem. B*, **2002**, 106, 1036.

52. Markovic, N., Gasteiger, H., Ross, P., *J. Phys. Chem.*, **1996**, 100, 6715.

53. Mentus, S., *Electrochim. Acta*, **2004**, 50, 27.

54. Ding, Z., Johnston, C., Zelenay, P., *ECS Transactions*, **2010**, 33, 565.

55. Manesh, K., Santhosh, P., Gopalan, A., Lee, K., *Electroanalysis*, **2006**, 18, 1564.

56. Leger, J., Koffi, K., Coutanceau, C., Lamy, C., *Proc. Electrochem. Soc.: (Electrocatalysis)*, **2006**, 2005-11, 295.